Journal of Applied Geophysics 105 (2014) 133–137

Contents lists available at ScienceDirect

Journal of Applied Geophysics

journal homepage: www.elsevier.com/locate/jappgeo

Displacement currents in geoelectromagnetic problems

Vladimir Mogilatov [a], Mark Goldman [b,*], Marina Persova [c], Yury Soloveichik [c]

[a] Institute of Petroleum Geology and Geophysics, Novosibirsk 630090, Russia
[b] University of Haifa, Haifa 31905, Israel
[c] The State Technical University of Novosibirsk, Novosibirsk 630073, Russia

ARTICLE INFO

Article history:
Received 17 December 2013
Accepted 17 March 2014
Available online 23 March 2014

Keywords:
Displacement currents
TE–TM fields
Time domain
Late times

ABSTRACT

The influence of displacement currents in conventional geoelectromagnetic (GEM) methods using unimodal transversal electric (TE) or multimodal TE and TM (transversal magnetic) fields is only significant at very high frequencies in the frequency domain or at extremely early times in the time domain. The transient process in the latter includes three stages: the propagation through air, the propagation through earth and the diffusion within the earth. The influence of displacement currents is significant mainly during the former two stages, normally up to several tens to a few hundreds of nanoseconds. The behavior is essentially different in novel GEM methods using a vertical electric dipole (VED) or circular electric dipole (CED) sources of unimodal TM-fields. Under certain geoelectric conditions, the influence of displacement currents in these methods might be crucial at late times as well. This happens, if the model consists of insulating layers. In the absence of displacement currents, such layers would totally mask underlying structures. However, TM-fields including displacement currents depend on geoelectric parameters below insulating layers at late times.

1. Introduction

In most cases, displacement currents (DSPC) are neglected when electromagnetic fields are applied for solving real geoexploration problems. Only in very high resistivity environments, such as permafrost, magmatic rocks, dry sands, carbonates, etc., the influence of DSPC might be significant at frequencies greater than roughly 100 kHz (Sinha, 1977). Such frequencies are only used in a very few existing methods such as RMT (radiomagnetotellurics). The situation in the time domain is even more severe since DSPC are significant at extremely early times in the order of nanoseconds, which are far beyond the working range of all existing transient electromagnetic (TEM) instruments. To the best of our knowledge, such a range has been realized in a single experimental TEM system developed in the framework of the Very Early Transient Electromagnetic (VETEM) project (Wright et al., 1996). However, the use of this system has never been moved beyond the experimental stage.

There is only one working geophysical method, in which DSPC play a crucial role. It is GPR (ground penetrating radar), which operates at frequencies greater than 25 MHz (e.g. Smith and Jol, 1995). At such frequencies, electromagnetic energy travels as waves in most environments and the measured signals are treated similarly to those in seismic methods. Therefore, GPR is not in the realm of inductive EM and as such it falls beyond the scope of this study.

Due to the lack to non-existence of practical applications in time domain EM, detailed theoretical investigations of DSPC based on numerical solutions for complicated 2D/3D models were mostly limited by frequency domain methods (e.g. Kalscheuer et al., 2008). There are very few studies in the time domain, which investigated the influence of DSPC on transient response based on numerical and/or analytical solutions and all them were carried out for relatively simple models (Bhattacharyya, 1959; Goldman et al., 1996; Wait, 1982; Weidelt, 2000).

To the best of our knowledge, all existing studies of DSPC both in frequency and time domains were carried out either for unimodal TE (transversal electric) fields or for bimodal TE–TM (transversal magnetic) fields. In recent years, there was an increasing interest in the use of unimodal TM-fields, which are highly sensitive to thin resistive structures and to lateral resistivity variations (e.g. Goldman and Mogilatov, 1978; Holten et al., 2009; Mogilatov and Balashov, 1996).

This study of DSPC includes both unimodal TE-fields generated by a vertical magnetic dipole (VMD) and unimodal TM-fields generated by a circular electric dipole (CED) on the surface of selected 1-D models. Note that a CED represents a surface analog of a more conventional vertical electric dipole (VED) source embedded within the earth (Mogilatov, 1992). The study led to unexpected results: contrary to unimodal TE-fields and multimodal TE–TM fields, which are only affected by DSPC at very shallow depths (early times), the influence of DSPC in unimodal

* Corresponding author at: University of Haifa, 199 Aba Khoushy Ave., Mount Carmel, Haifa, Israel. Tel.: +972 8 9751713.
E-mail address: mgol1302@gmail.com (M. Goldman).

http://dx.doi.org/10.1016/j.jappgeo.2014.03.014
0926-9851/

TM-fields might be significant and even crucial at large depths (late times) as well.

2. VMD (TE-field), early times (high frequencies)

Let's consider a model consisting of a boundary ($z = 0$) between two homogeneous half spaces with arbitrary resistivities and dielectric permittivities. The magnetic permeability in both half spaces equals that in vacuum. A VMD having moment M_z is located in the upper half space at point $z = z_0$ of a cylindrical coordinate system with the z-axes pointed up (Fig. 1a). At time instant $t = 0$, the moment abruptly drops to zero. The analytical solution in frequency domain is well known (e.g. Wait, 1982). In fact, it is identical to that in the quasi-static approximation with the only difference in the expressions for wave numbers:

$$k_i^2 = -\mathbf{i}\omega\mu_0/\rho_i - \omega^2\mu_0\varepsilon_i, \tag{1}$$

$$k_i^2 = -\mathbf{i}\omega\mu_0/\rho_i (i = 0, 1). \tag{2}$$

Here Eq. (1) represents wave numbers including DSPC and Eq. (2) represents wave numbers in the quasi-static limit. Such an insignificant difference in the frequency domain makes it extremely difficult up to impossible to perform a numerical Fourier transform into the time domain. Fortunately, the solution in time domain for the model under consideration, can be obtained analytically using the Laplace transform by substituting $\mathbf{i}\omega = \gamma_i - s$, $\gamma_i = 1/(2\rho_i\varepsilon_i)$, $i = 0, 1$.

Let's consider the practically interesting case, when VMD is located on the surface of a homogeneous earth ($z_0 = 0$). This problem has been considered by Bhattacharyya (1959). However, our solution considerably differs from that of Bhattacharyya (1959) by the appearance of a leading edge with infinitely large amplitude (point source, ideal step-off excitation). By applying the Laplace transform to the full frequency domain solution, one obtains the following equations for electrical and vertical magnetic fields, E_ϕ and dB_z/dt, respectively (Goldman et al., 1996):

$$E_\phi = \frac{M_z\mu_0}{2\pi}(A_1 - A_0), \tag{3}$$

where

$$A_i = \frac{\overline{\rho}}{\mu_0}\cdot\frac{T_i^2}{r^4}\cdot\left[\int_{-\infty}^{\infty}\left(I_i^{(2)}\cdot T_i - I_i^{(1)}\right)\cdot U(\tau - T)\cdot\varphi_i(\tau)\cdot U(t-\tau)\cdot d\tau + \right.$$
$$+\varphi_i(T_i)\cdot\left(1+\frac{\gamma_i^2T_i^2}{2}\right)\cdot U(t-T_i) - \varphi_{i\tau}'(T_i)\cdot T_i\cdot U(t-T_i) + \tag{4}$$
$$\left.+\varphi_i(T_i)\cdot T_i\cdot\delta(t-T_i)\right].$$

$U(x)$ and $\delta(x)$ are the Heaviside step-off function and the Dirac delta function, respectively, $I^{(n)}$ is the n-th derivative of $I_i \equiv I_i^{(0)} = I_0\left(\gamma_i\sqrt{\tau^2 - T_i^2}\right.$ with respect to T, I_0 is the modified Bessel function of zero order, $T_i = r/c_i$ is the first arrival time, $c = 1/\sqrt{\mu_0\varepsilon_i}$ is the light velocity in the i-th medium,

$$\varphi_i(\tau) = -\frac{\exp(-\gamma_i\tau)}{\tau^2}\cdot\{1 + \gamma_i\tau + \exp[-2\overline{\gamma}(t-\tau)]\cdot(2\overline{\gamma}\tau - \gamma_i\tau - 1)\},$$
$$\overline{\gamma} = 1/(2\overline{\rho\varepsilon}), \overline{\varepsilon} = \varepsilon_1 - \varepsilon_0, \overline{\rho} = \rho_0\rho_1/(\rho_0 - \rho_1), i = 0, 1.$$

These equations are suitable for calculations. The equations are further simplified by considering the practically important case, when the upper half space is air ($\rho_0 = \infty$). Then $\gamma_0 = 0$ and the expression for A_0 in Eq. (4) becomes:

$$A_0 = \frac{\overline{\rho}}{\mu_0}\cdot\frac{T_0^2}{r^4}\left[\phi_0(T_0)U(t-T_0) - \varphi_{0\tau}'(T_0)T_0U(t-T_0) + \varphi_0(T_0)T_0\delta(t-T_0)\right]. \tag{5}$$

The expression for the time derivative of the vertical magnetic field is obtained from Eq. (3) by simple differentiation:

$$\dot{B}_z = -\left(\frac{1}{r} + \frac{\partial}{\partial r}\right)\cdot E_\varphi. \tag{6}$$

Fig. 2 shows the transient responses of E_ϕ for different relative dielectric permittivities $\varepsilon_1/\varepsilon_0$ of the earth. It is important to emphasize that the responses are calculated for the ideal point source and step

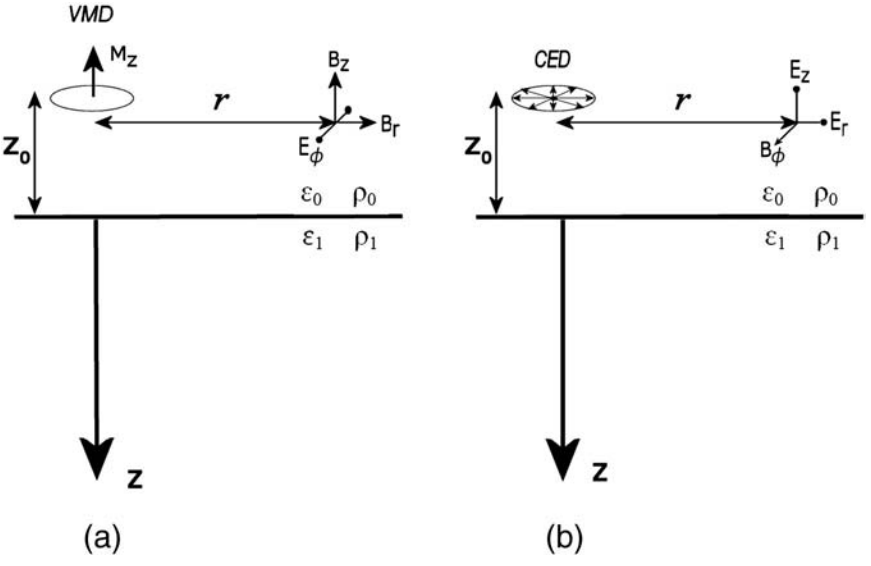

Fig. 1. Model geometry.

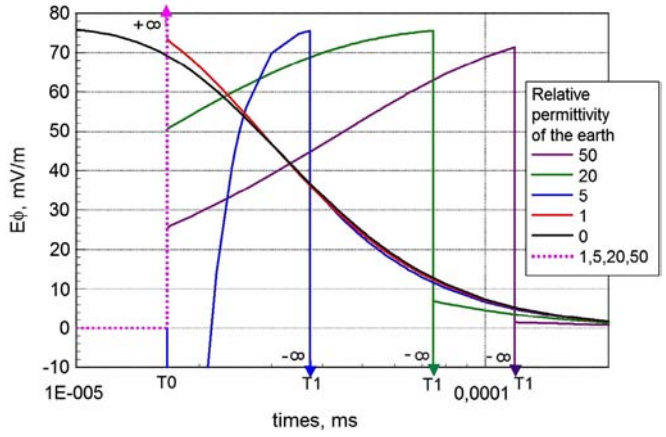

Fig. 2. E_ϕ transient response of VMD for different relative dielectric permittivities of earth. The model is shown in Fig. 1, where $z_0 = 0$, $r = 5$ m, $\rho_1 = 100$ Ω-m.

function excitation. The whole transient process is clearly divided by two singular points, $t = T_0$ (first arrival through air) and $t = T_1$ (first arrival through earth), into three different stages. During the first stage, $0 < t < T_0$, the electromagnetic energy has not arrived yet to the measurement point and, as a result, $E_\phi = 0$. At instant $t = T_0 = 16.678$ ns, E_ϕ changes from 0 to ∞ and instantly drops to some final positive or negative value depending on $\varepsilon_1/\varepsilon_0$ (in Fig. 2, only $\varepsilon_1/\varepsilon_0 = 5$ drops to a negative value). During the second stage, $T_0 < t < T_1$, the field gradually increases to a value depending on ρ_1 and ε_1. This process is caused by the energy arriving through air. At instant $t = T_1 = r \cdot \sqrt{\mu_0 \varepsilon_1}$, the energy arrives through earth and E_ϕ changes to $-\infty$ for all $\varepsilon_1/\varepsilon_0 > 1$ and returns to some final value either positive or negative depending on ρ_1 and ε_1. After that instant, the field gradually approaches its quasi-static behavior, $\varepsilon_1/\varepsilon_0 = 0$. In the specific case of $\varepsilon_1/\varepsilon_0 = 1$, the energy arrives through air and earth simultaneously ($T_0 = T_1$). At this instant, E_ϕ only changes to $+\infty$ and returns to the value close to the quasi-static one.

It should be noted that the appearance of the instantaneous infinite field values is caused by the use of such abstract idealized patterns as point source and step function.

3. CED (TM-field), early times (high frequencies)

There are two conventional sources of a unimodal TM-field: a toroidal coil (pure inductive excitation) and a vertical electric dipole (mixed galvanic/inductive excitation). Since both conventional sources are hard to apply in the field, a more practical surface analog of VED has been recently developed (Mogilatov, 1996). This novel source of a unimodal TM-field called a circular electric dipole (CED) is considered in this study (Fig. 1b).

There are three different modes of CEDs, two theoretical and one practical. Both theoretical modes imply the following distribution of a non-zero extrinsic radial current density, j_r, along a circle of radius, r_0:

$$j_r^{cm}(r) = \frac{I}{2\pi r} \cdot [U(r - r_0 + dr_0/2) - U(r - r_0 - dr_0/2)], \tag{7}$$

where $U(x)$ is the Heaviside function (Fig. 3, left and right).

The difference between the theoretical modes is in the nature of the central electrode. It could be either a point electrode (Fig. 3, left), or an extrinsic radial current density uniformly distributed along a circle of radius, a ($a < r_0$, Fig. 3, right). In fact, the former mode is a particular case of the latter mode with $a = 0$. The practical mode of a CED shown in Fig. 3 (center) includes a final number of radial electric lines with a common central electrode. It was found empirically that the practical mode adequately represents the theoretical mode shown in Fig. 3 (left), if the minimum number of radial electric lines equals eight (Mogilatov and Balashov, 1996). This mode has been successfully applied in the field contouring oil and gas reservoirs and kimberlite pipes (Mogilatov et al., 2009).

Due to cylindrical symmetry, a CED generates the following EM components in an arbitrary 1-D horizontally layered earth: E_r, E_z and H_φ. Applying the standard method of separation of variables, one obtains the following solution for the E_r-component (at $z \le 0$) of a CED source in frequency domain for the same model described above (Mogilatov, 1996):

$$E_r(\omega) = \frac{I_0 b^2}{8\pi\hat{\sigma}_1} \cdot \frac{\partial^3}{\partial z^2 \partial r} \left\{ \frac{1}{R} \cdot e^{-k_1 R} \right\}, \tag{8}$$

where $\widetilde{\sigma}_1 = \sigma_1 + \mathbf{i}\omega\varepsilon_1$. Substituting $\mathbf{i}\omega = \gamma_i - s$, $\gamma_i = 1/(2\rho_i\varepsilon_i)$, $i = 0, 1$ and applying to Eq. (8) the integral Laplace transform, one obtains the following expression in time domain for $z = 0$.

$$\begin{aligned} E_r(t) = \overline{E}_r + \frac{I_0 b^2}{8\pi\sigma_1} \frac{T_1^2}{r^4} \Bigg[& \int_{-\infty}^{\infty} \left(I^{(2)} T_1 - I^{(1)} \right) U(\tau - T_1) \varphi(\tau) U(t - \tau) d\tau + \\ & + \varphi(T_1) \left(1 + \frac{\gamma_1^2 T_1^2}{2} \right) U(t - T_1) - \varphi'_\tau(T_1) T_1 U(t - T_1) \\ & + \varphi(T_1) T_1 \delta(t - T_1) \Bigg], \end{aligned} \tag{9}$$

where all designations are identical to those used in the previous Section. Contrary to the numerical Fourier transform of Eq. (8), Eq. (9) is suitable for calculations.

The results of the calculations are shown in Fig. 4. Contrary to the VMD (Fig. 2), the response from the CED starts at $t = T_1$, where T_1 is the first arrival time through earth, $T_1 = r\sqrt{\mu_0\varepsilon_1}$. At times $t < T_1$, the signal has its DC value, the same as at times $t \le 0$. At times $t > T_1$, the signal decays gradually approaching its quasi-static behavior. At instant $t = T_1$, the response becomes infinitely large, but such a behavior is caused by using a dipole source and ideal step-function excitation. In

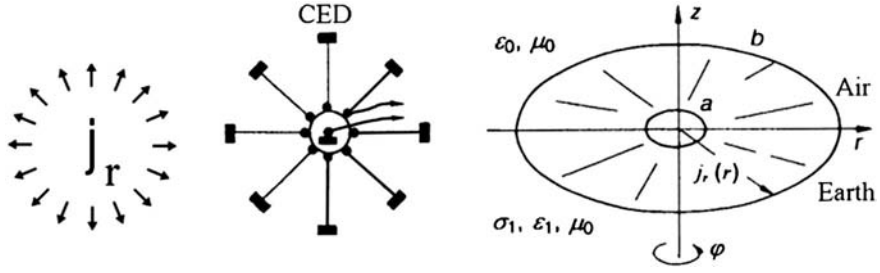

Fig. 3. Theoretical (left), practical (center) and idealized (right) circular electric dipoles (CEDs). The theoretical and practical CEDs are shown from above. The idealized CED is shown from the side.

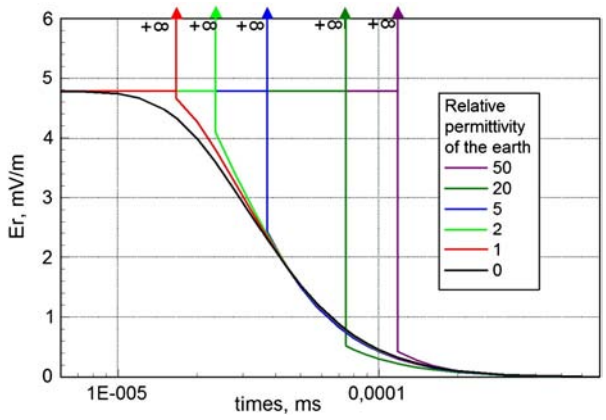

Fig. 4. E_r transient response of a CED for different relative dielectric permittivities of earth. The model is shown in Fig. 1, where $z_0 = 0$, $r = 5$ m, $\rho_1 = 100$ Ω-m.

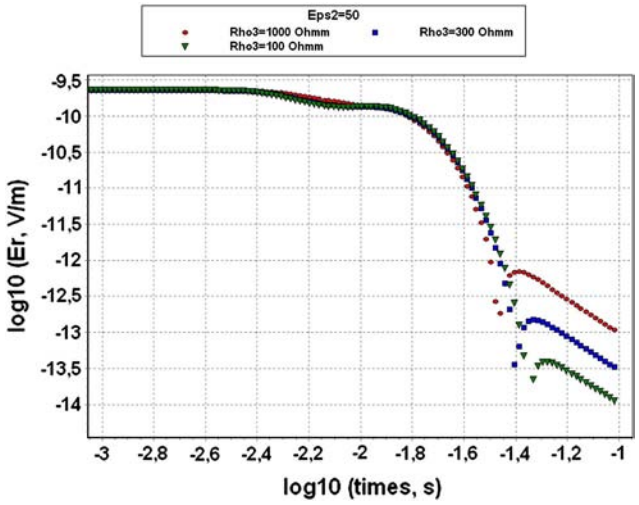

Fig. 6. Transient responses of the E_r-component of a CED for different resistivities of the layer underlying the insulating dielectric layer. The model is shown in Fig. 5a.

case of finite dimensions of the CED and finite duration of step off excitation, the singularity at the first arrival time disappears.

Comparison of Figs. 2 and 4 shows that the main difference between the VMD (TE-field) and CED (TM-field) at very early times manifests itself in the absence of a signal arriving from CED to a receiver through air. In other words, a unimodal TM-field transmitter does not emit electromagnetic energy into the air.

4. CED (TM-field) late times (deep soundings)

The influence of DSPC in geoelectromagnetic methods using conventional unimodal TE-fields or multimodal TE/TM-fields is limited by extremely early times (high frequencies) affecting shallow exploration depth only. However, under certain geoelectric conditions it is not the case for a unimodal TM-field. Such conditions take place in the presence of a thin resistive (more precisely, insulating) layer. In case of a DC unimodal TM-field, such a layer shields the underlying structures. Similar behavior is observed for EM unimodal TM-field (e.g. of VED or CED) under a quasi-static approximation. However, the situation becomes entirely different, if DSPC are taken into account within the insulating layer.

Fig. 5b shows the responses of the E_r-component for the model presented in Fig. 5a for different relative dielectric permittivities. While the quasi-static response ($\varepsilon_2 = 0$) monotonically decreases from a DC value at early times to a quasi-exponential decay at late times, the responses including DSPC underwent sign reversal, after which they decay at late times much slower than in the quasi-static case. The responses are perfectly resolved with regard to the dielectric permittivity of the layer.

The calculations were carried out using two different algorithms: the 3-D finite element algorithm (Persova et al., 2011) modified for calculating 1-D responses and the standard algorithm using the numerical Fourier transform of the frequency response, which turned out fairly accurate for the model in question in the considered time range.

Fig. 6 shows excellent resolution of the signal with regard to the resistivity of the underlying layer. Although the resolution takes place at relatively late times (after the sign reversals), the amplitudes of the signals are not as small as they would be in the quasi-static case (see Fig. 5(b) for $\varepsilon_2 = 0$). In other words, the dielectric permittivity of an

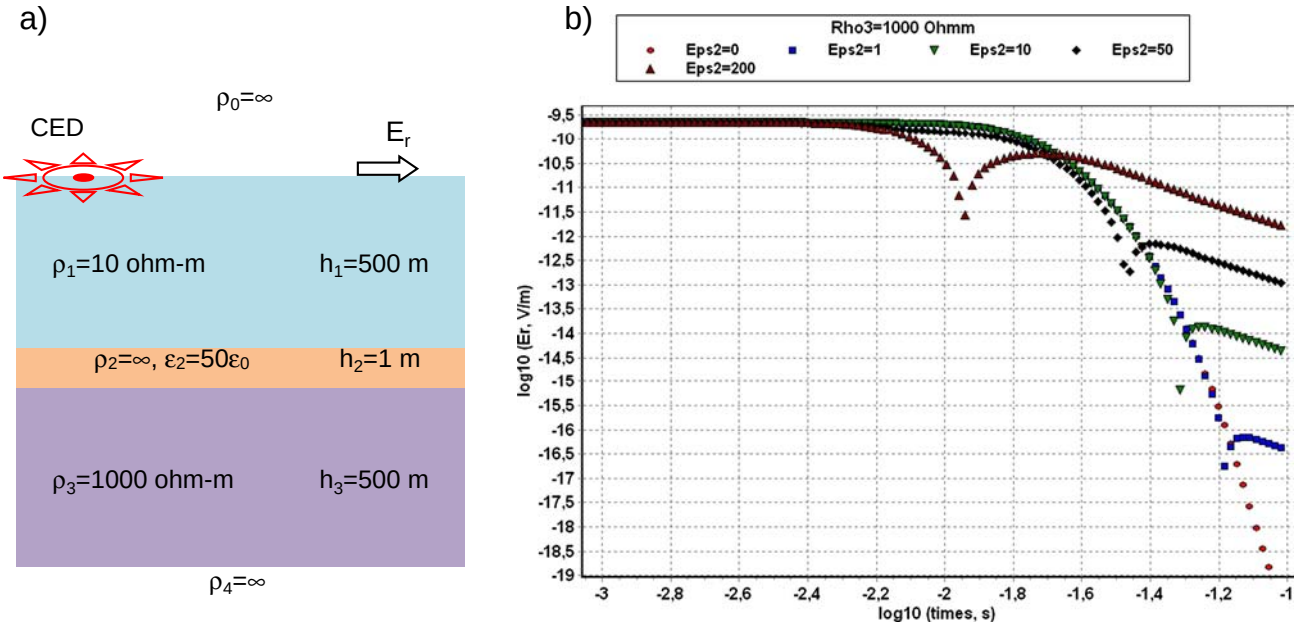

Fig. 5. a) Model; b) Transient responses of the Er-component for different dielectric permittivities of the insulating layer. The CED radius = 500 m; the offset = 2000 m.

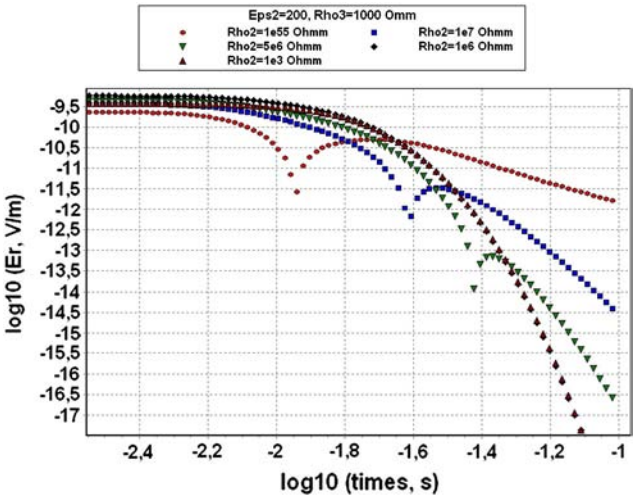

Fig. 7. Transient responses of the E_r-component of a CED for different resistivities of the thin dielectric layer. The model is shown in Fig. 5a.

insulating layer enhances the sensitivity of a unimodal TM-field to the resistivity of the underlying material. This result is rather unexpected taking into account the following two commonly accepted facts:

1). Within quasi-static limits, insulating layers totally mask underlying resistivities in case of unimodal TM-fields.

2). Traditionally, displacement currents (DSPC) are expected to be significant at very early times only.

The above phenomenon is found for a perfectly insulating material, which is never encountered in geology. The highest resistivities measured on samples of some igneous and metamorphic rocks (e.g. granite, basalts, quartzite) roughly vary between 10^6 and 10^8 Ω-m (e.g. Keller and Frischknecht, 1966). Within the earth, these rocks normally have lower resistivities due to weathering, humidity, etc. Therefore it is important to find out how a finite resistivity of the dielectric layer affects the influence of DSPC at late times. Fig. 7 shows the responses calculated for the model presented in Fig. 5a for different resistivities of the thin dielectric layer. It can be seen that there is a threshold value of the resistivity roughly around 10^6 Ω-m, below which the influence of DSPC disappears and the thin resistive layer behaves as a screen with regard to the underlying structures. Thus in practice, the discovered effect might be applicable only in very special exploration problems, in which artificial materials such as plastic, are involved. One of such problems is detecting and mapping leaks from waste disposal sites lined with synthetic materials (Boryta and Nabighian, 1985).

5. Conclusions

At very high frequencies and super early times, displacement currents play a significant role in all kinds of fields: unimodal TE- and TM-fields and multimodal fields. However, the propagation of TM-fields is essentially different because the TM-sources (CED or VED) do not generate a field in air and the electromagnetic energy arrives to a receiver through the conductive earth only.

Contrary to a quasi-static case, time domain calculations including propagation effects cannot be carried out using the traditional numerical Fourier transform of a frequency response including displacement currents. The appropriate mathematical apparatus should be significantly modified.

At low frequencies and late times, displacement currents might be also significant, but only in the case of TM-fields and in models including insulating layers. Calculations show that this effect disappears, if the resistivity of the latter drops below some threshold value (roughly in the order of 10^6 Ω-m). Thus, the discovered phenomenon is mainly of a theoretical interest and can be only applied in geophysical practice, when some man-made materials are involved (e.g. in the exploration of lined waste disposal sites).

Acknowledgments

Our thanks are due to James Macnae and Colin Farquharson for their useful comments and suggestions and for the positive assessment of our results.

References

Bhattacharyya, B.K., 1959. Electromagnetic fields of a transient magnetic dipole on the earth's surface. Geophysics 24, 89–108.
Boryta, D.A., Nabighian, M.N., 1985. Method for determining a leak in a pond liner of electrically insulating material, U.S. Patent no. 4.543.525.
Goldman, M., Mogilatov, V., 1978. Transient field of a vertical electric dipole embedded in a horizontally layered half-space (in Russian). Theory and Applications of Electromagnetic Fields in Geophysical Exploration. Academy of Science of the USSR, Siberian Branch, pp. 123–138.
Goldman, M., Mogilatov, V., Rabinovich, M., 1996. Transient response of a homogeneous half space with due regard for displacement currents. J. Appl. Geophys. 37, 291–305.
Holten, T., Flekkøy, E.G., Måløy, K.J., Singer, B., 2009. Vertical source and receiver CSEM method in time-domain. SEG Annual Meeting, Houston, Texas, Expanded Abstracts, pp. 749–752.
Kalscheuer, T., Pedersen, L.B., Siripunvaraporn, W., 2008. Radiomagnetotelluric two-dimensional forward and inverse modelling accounting for displacement currents. 175, 486–514.
Keller, G.V., Frischknecht, F.C., 1966. Electrical Methods in Geophysical Prospecting. Pergamon Press (519 pp.).
Mogilatov, V., 1992. A circular electric dipole as a new source in electric surveys. Izvestiya. Phys. Solid Earth 6, 97–105.
Mogilatov, V., 1996. Excitation of a half-space by a radial current sheet source. Pure Appl. Geophys. 147, 763–775.
Mogilatov, V., Balashov, B., 1996. A new method of geoelectrical prospecting by vertical electric current soundings. J. Appl. Geophys. 36, 31–41.
Mogilatov, V., Mukhopadhyay, P., Mallick, S., 2009. An advanced deep penetrating EM technique for hydrocarbon and mineral exploration: mVECS. NGF Abstracts and Proceedings, 3 pp. 21–24.
Persova, M.G., Soloveichik, Yu.G., Trigubovich, G.M., 2011. Computer modeling of geoelectromagnetic fields in three dimensional media by the finite element method. Izvestiya. Phys. Solid Earth 47, 79–89.
Sinha, A.K., 1977. Influence of altitude and displacement currents on plane-wave EM-fields. Geophysics 42, 77–91.
Smith, D.G., Jol, H.M., 1995. Ground penetrating radar: antenna frequencies and maximum probable depth of penetration in Quaternary sediments. J. Appl. Geophys. 33, 93–100.
Wait, J.R., 1982. Geoelectromagnetism. Academic Press (268 pp.).
Weidelt, P., 2000. Electromagnetic edge diffraction revisited: the transient field of magnetic dipole sources. Geophys. J. Int. 141, 605–622.
Wright, D.L., Grover, T.P., Labson, V.F., 1996. The Very Early Time Electromagnetic (VETEM) system: first field test results. Extended Abstracts, 9th EEGS Symposium on the Application of Geophysics to Engineering and Environmental Problems.